arXiv:0808.0017v1 [hep-ex] 31 Jul 2008

Search for Invisible Decays of a Light Scalar in Radiative Transitions $\Upsilon(3S) \to \gamma A^0$

The BABAR Collaboration

July 31, 2008

Abstract

We search for a light scalar particle produced in single-photon decays of the $\Upsilon(3S)$ resonance through the process $\Upsilon(3S) \to \gamma + A^0$, $A^0 \to$ invisible. Such an object appears in Next-to-Minimal Supersymmetric extensions of the Standard Model, where a light CP-odd Higgs boson naturally couples strongly to b-quarks. If, in addition, there exists a light, stable neutralino, decays of A^0 could be preferentially to an invisible final state. We search for events with a single high-energy photon and a large missing mass, consistent with a 2-body decay of $\Upsilon(3S)$. We find no evidence for such processes in a sample of 122×10^6 $\Upsilon(3S)$ decays collected by the BABAR collaboration at the PEP-II B-factory, and set 90% C.L. upper limits on the branching fraction $\mathcal{B}(\Upsilon(3S) \to \gamma A^0) \times \mathcal{B}(A^0 \to \text{invisible})$ at $(0.7 - 31) \times 10^{-6}$ in the mass range $m_{A^0} \leq 7.8$ GeV. The results are preliminary.

Submitted to the 34th International Conference on High-Energy Physics, ICHEP 08,
29 July—5 August 2008, Philadelphia, Pennsylvania.

The *BABAR* Collaboration,

B. Aubert, M. Bona, Y. Karyotakis, J. P. Lees, V. Poireau, E. Prencipe, X. Prudent, V. Tisserand

Laboratoire de Physique des Particules, IN2P3/CNRS et Université de Savoie, F-74941 Annecy-Le-Vieux, France

J. Garra Tico, E. Grauges

Universitat de Barcelona, Facultat de Fisica, Departament ECM, E-08028 Barcelona, Spain

L. Lopez[ab], A. Palano[ab], M. Pappagallo[ab]

INFN Sezione di Bari[a]; Dipartmento di Fisica, Università di Bari[b], I-70126 Bari, Italy

G. Eigen, B. Stugu, L. Sun

University of Bergen, Institute of Physics, N-5007 Bergen, Norway

G. S. Abrams, M. Battaglia, D. N. Brown, R. N. Cahn, R. G. Jacobsen, L. T. Kerth, Yu. G. Kolomensky, G. Lynch, I. L. Osipenkov, M. T. Ronan,[1] K. Tackmann, T. Tanabe

Lawrence Berkeley National Laboratory and University of California, Berkeley, California 94720, USA

C. M. Hawkes, N. Soni, A. T. Watson

University of Birmingham, Birmingham, B15 2TT, United Kingdom

H. Koch, T. Schroeder

Ruhr Universität Bochum, Institut für Experimentalphysik 1, D-44780 Bochum, Germany

D. Walker

University of Bristol, Bristol BS8 1TL, United Kingdom

D. J. Asgeirsson, B. G. Fulsom, C. Hearty, T. S. Mattison, J. A. McKenna

University of British Columbia, Vancouver, British Columbia, Canada V6T 1Z1

M. Barrett, A. Khan

Brunel University, Uxbridge, Middlesex UB8 3PH, United Kingdom

V. E. Blinov, A. D. Bukin, A. R. Buzykaev, V. P. Druzhinin, V. B. Golubev, A. P. Onuchin, S. I. Serednyakov, Yu. I. Skovpen, E. P. Solodov, K. Yu. Todyshev

Budker Institute of Nuclear Physics, Novosibirsk 630090, Russia

M. Bondioli, S. Curry, I. Eschrich, D. Kirkby, A. J. Lankford, P. Lund, M. Mandelkern, E. C. Martin, D. P. Stoker

University of California at Irvine, Irvine, California 92697, USA

S. Abachi, C. Buchanan

University of California at Los Angeles, Los Angeles, California 90024, USA

J. W. Gary, F. Liu, O. Long, B. C. Shen,[1] G. M. Vitug, Z. Yasin, L. Zhang

University of California at Riverside, Riverside, California 92521, USA

---

[1]Deceased

2

V. Sharma

University of California at San Diego, La Jolla, California 92093, USA

C. Campagnari, T. M. Hong, D. Kovalskyi, M. A. Mazur, J. D. Richman

University of California at Santa Barbara, Santa Barbara, California 93106, USA

T. W. Beck, A. M. Eisner, C. J. Flacco, C. A. Heusch, J. Kroseberg, W. S. Lockman, A. J. Martinez,
T. Schalk, B. A. Schumm, A. Seiden, M. G. Wilson, L. O. Winstrom

University of California at Santa Cruz, Institute for Particle Physics, Santa Cruz, California 95064, USA

C. H. Cheng, D. A. Doll, B. Echenard, F. Fang, D. G. Hitlin, I. Narsky, T. Piatenko, F. C. Porter

California Institute of Technology, Pasadena, California 91125, USA

R. Andreassen, G. Mancinelli, B. T. Meadows, K. Mishra, M. D. Sokoloff

University of Cincinnati, Cincinnati, Ohio 45221, USA

P. C. Bloom, W. T. Ford, A. Gaz, J. F. Hirschauer, M. Nagel, U. Nauenberg, J. G. Smith, K. A. Ulmer,
S. R. Wagner

University of Colorado, Boulder, Colorado 80309, USA

R. Ayad,[2] A. Soffer,[3] W. H. Toki, R. J. Wilson

Colorado State University, Fort Collins, Colorado 80523, USA

D. D. Altenburg, E. Feltresi, A. Hauke, H. Jasper, M. Karbach, J. Merkel, A. Petzold, B. Spaan, K. Wacker

Technische Universität Dortmund, Fakultät Physik, D-44221 Dortmund, Germany

M. J. Kobel, W. F. Mader, R. Nogowski, K. R. Schubert, R. Schwierz, A. Volk

Technische Universität Dresden, Institut für Kern- und Teilchenphysik, D-01062 Dresden, Germany

D. Bernard, G. R. Bonneaud, E. Latour, M. Verderi

Laboratoire Leprince-Ringuet, CNRS/IN2P3, Ecole Polytechnique, F-91128 Palaiseau, France

P. J. Clark, S. Playfer, J. E. Watson

University of Edinburgh, Edinburgh EH9 3JZ, United Kingdom

M. Andreotti[ab], D. Bettoni[a], C. Bozzi[a], R. Calabrese[ab], A. Cecchi[ab], G. Cibinetto[ab], P. Franchini[ab],
E. Luppi[ab], M. Negrini[ab], A. Petrella[ab], L. Piemontese[a], V. Santoro[ab]

INFN Sezione di Ferrara[a]; Dipartimento di Fisica, Università di Ferrara[b], I-44100 Ferrara, Italy

R. Baldini-Ferroli, A. Calcaterra, R. de Sangro, G. Finocchiaro, S. Pacetti, P. Patteri, I. M. Peruzzi,[4]
M. Piccolo, M. Rama, A. Zallo

INFN Laboratori Nazionali di Frascati, I-00044 Frascati, Italy

A. Buzzo[a], R. Contri[ab], M. Lo Vetere[ab], M. M. Macri[a], M. R. Monge[ab], S. Passaggio[a], C. Patrignani[ab],
E. Robutti[a], A. Santroni[ab], S. Tosi[ab]

INFN Sezione di Genova[a]; Dipartimento di Fisica, Università di Genova[b], I-16146 Genova, Italy

---

[2]Now at Temple University, Philadelphia, Pennsylvania 19122, USA
[3]Now at Tel Aviv University, Tel Aviv, 69978, Israel
[4]Also with Università di Perugia, Dipartimento di Fisica, Perugia, Italy

K. S. Chaisanguanthum, M. Morii

Harvard University, Cambridge, Massachusetts 02138, USA

A. Adametz, J. Marks, S. Schenk, U. Uwer

Universität Heidelberg, Physikalisches Institut, Philosophenweg 12, D-69120 Heidelberg, Germany

V. Klose, H. M. Lacker

Humboldt-Universität zu Berlin, Institut für Physik, Newtonstr. 15, D-12489 Berlin, Germany

D. J. Bard, P. D. Dauncey, J. A. Nash, M. Tibbetts

Imperial College London, London, SW7 2AZ, United Kingdom

P. K. Behera, X. Chai, M. J. Charles, U. Mallik

University of Iowa, Iowa City, Iowa 52242, USA

J. Cochran, H. B. Crawley, L. Dong, W. T. Meyer, S. Prell, E. I. Rosenberg, A. E. Rubin

Iowa State University, Ames, Iowa 50011-3160, USA

Y. Y. Gao, A. V. Gritsan, Z. J. Guo, C. K. Lae

Johns Hopkins University, Baltimore, Maryland 21218, USA

N. Arnaud, J. Béquilleux, A. D'Orazio, M. Davier, J. Firmino da Costa, G. Grosdidier, A. Höcker,
V. Lepeltier, F. Le Diberder, A. M. Lutz, S. Pruvot, P. Roudeau, M. H. Schune, J. Serrano, V. Sordini,[5]
A. Stocchi, G. Wormser

Laboratoire de l'Accélérateur Linéaire, IN2P3/CNRS et Université Paris-Sud 11, Centre Scientifique d'Orsay, B. P. 34, F-91898 Orsay Cedex, France

D. J. Lange, D. M. Wright

Lawrence Livermore National Laboratory, Livermore, California 94550, USA

I. Bingham, J. P. Burke, C. A. Chavez, J. R. Fry, E. Gabathuler, R. Gamet, D. E. Hutchcroft, D. J. Payne,
C. Touramanis

University of Liverpool, Liverpool L69 7ZE, United Kingdom

A. J. Bevan, C. K. Clarke, K. A. George, F. Di Lodovico, R. Sacco, M. Sigamani

Queen Mary, University of London, London, E1 4NS, United Kingdom

G. Cowan, H. U. Flaecher, D. A. Hopkins, S. Paramesvaran, F. Salvatore, A. C. Wren

University of London, Royal Holloway and Bedford New College, Egham, Surrey TW20 0EX, United Kingdom

D. N. Brown, C. L. Davis

University of Louisville, Louisville, Kentucky 40292, USA

A. G. Denig M. Fritsch, W. Gradl, G. Schott

Johannes Gutenberg-Universität Mainz, Institut für Kernphysik, D-55099 Mainz, Germany

---

[5]Also with Università di Roma La Sapienza, I-00185 Roma, Italy

4

K. E. Alwyn, D. Bailey, R. J. Barlow, Y. M. Chia, C. L. Edgar, G. Jackson, G. D. Lafferty, T. J. West, J. I. Yi

University of Manchester, Manchester M13 9PL, United Kingdom

J. Anderson, C. Chen, A. Jawahery, D. A. Roberts, G. Simi, J. M. Tuggle

University of Maryland, College Park, Maryland 20742, USA

C. Dallapiccola, X. Li, E. Salvati, S. Saremi

University of Massachusetts, Amherst, Massachusetts 01003, USA

R. Cowan, D. Dujmic, P. H. Fisher, G. Sciolla, M. Spitznagel, F. Taylor, R. K. Yamamoto, M. Zhao

Massachusetts Institute of Technology, Laboratory for Nuclear Science, Cambridge, Massachusetts 02139, USA

P. M. Patel, S. H. Robertson

McGill University, Montréal, Québec, Canada H3A 2T8

A. Lazzaro[ab], V. Lombardo[a], F. Palombo[ab]

INFN Sezione di Milano[a]; Dipartimento di Fisica, Università di Milano[b], I-20133 Milano, Italy

J. M. Bauer, L. Cremaldi R. Godang,[6] R. Kroeger, D. A. Sanders, D. J. Summers, H. W. Zhao

University of Mississippi, University, Mississippi 38677, USA

M. Simard, P. Taras, F. B. Viaud

Université de Montréal, Physique des Particules, Montréal, Québec, Canada H3C 3J7

H. Nicholson

Mount Holyoke College, South Hadley, Massachusetts 01075, USA

G. De Nardo[ab], L. Lista[a], D. Monorchio[ab], G. Onorato[ab], C. Sciacca[ab]

INFN Sezione di Napoli[a]; Dipartimento di Scienze Fisiche, Università di Napoli Federico II[b], I-80126 Napoli, Italy

G. Raven, H. L. Snoek

NIKHEF, National Institute for Nuclear Physics and High Energy Physics, NL-1009 DB Amsterdam, The Netherlands

C. P. Jessop, K. J. Knoepfel, J. M. LoSecco, W. F. Wang

University of Notre Dame, Notre Dame, Indiana 46556, USA

G. Benelli, L. A. Corwin, K. Honscheid, H. Kagan, R. Kass, J. P. Morris, A. M. Rahimi, J. J. Regensburger, S. J. Sekula, Q. K. Wong

Ohio State University, Columbus, Ohio 43210, USA

N. L. Blount, J. Brau, R. Frey, O. Igonkina, J. A. Kolb, M. Lu, R. Rahmat, N. B. Sinev, D. Strom, J. Strube, E. Torrence

University of Oregon, Eugene, Oregon 97403, USA

---

[6]Now at University of South Alabama, Mobile, Alabama 36688, USA

5

G. Castelli[ab], N. Gagliardi[ab], M. Margoni[ab], M. Morandin[a], M. Posocco[a], M. Rotondo[a], F. Simonetto[ab], R. Stroili[ab], C. Voci[ab]

INFN Sezione di Padova[a]; Dipartimento di Fisica, Università di Padova[b], I-35131 Padova, Italy

P. del Amo Sanchez, E. Ben-Haim, H. Briand, G. Calderini, J. Chauveau, P. David, L. Del Buono, O. Hamon, Ph. Leruste, J. Ocariz, A. Perez, J. Prendki, S. Sitt

Laboratoire de Physique Nucléaire et de Hautes Energies, IN2P3/CNRS, Université Pierre et Marie Curie-Paris6, Université Denis Diderot-Paris7, F-75252 Paris, France

L. Gladney

University of Pennsylvania, Philadelphia, Pennsylvania 19104, USA

M. Biasini[ab], R. Covarelli[ab], E. Manoni[ab],

INFN Sezione di Perugia[a]; Dipartimento di Fisica, Università di Perugia[b], I-06100 Perugia, Italy

C. Angelini[ab], G. Batignani[ab], S. Bettarini[ab], M. Carpinelli[ab],[7] A. Cervelli[ab], F. Forti[ab], M. A. Giorgi[ab], A. Lusiani[ac], G. Marchiori[ab], M. Morganti[ab], N. Neri[ab], E. Paoloni[ab], G. Rizzo[ab], J. J. Walsh[a]

INFN Sezione di Pisa[a]; Dipartimento di Fisica, Università di Pisa[b]; Scuola Normale Superiore di Pisa[c], I-56127 Pisa, Italy

D. Lopes Pegna, C. Lu, J. Olsen, A. J. S. Smith, A. V. Telnov

Princeton University, Princeton, New Jersey 08544, USA

F. Anulli[a], E. Baracchini[ab], G. Cavoto[a], D. del Re[ab], E. Di Marco[ab], R. Faccini[ab], F. Ferrarotto[a], F. Ferroni[ab], M. Gaspero[ab], P. D. Jackson[a], L. Li Gioi[a], M. A. Mazzoni[a], S. Morganti[a], G. Piredda[a], F. Polci[ab], F. Renga[ab], C. Voena[a]

INFN Sezione di Roma[a]; Dipartimento di Fisica, Università di Roma La Sapienza[b], I-00185 Roma, Italy

M. Ebert, T. Hartmann, H. Schröder, R. Waldi

Universität Rostock, D-18051 Rostock, Germany

T. Adye, B. Franek, E. O. Olaiya, F. F. Wilson

Rutherford Appleton Laboratory, Chilton, Didcot, Oxon, OX11 0QX, United Kingdom

S. Emery, M. Escalier, L. Esteve, S. F. Ganzhur, G. Hamel de Monchenault, W. Kozanecki, G. Vasseur, Ch. Yèche, M. Zito

CEA, Irfu, SPP, Centre de Saclay, F-91191 Gif-sur-Yvette, France

X. R. Chen, H. Liu, W. Park, M. V. Purohit, R. M. White, J. R. Wilson

University of South Carolina, Columbia, South Carolina 29208, USA

M. T. Allen, D. Aston, R. Bartoldus, P. Bechtle, J. F. Benitez, R. Cenci, J. P. Coleman, M. R. Convery, J. C. Dingfelder, J. Dorfan, G. P. Dubois-Felsmann, W. Dunwoodie, R. C. Field, A. M. Gabareen, S. J. Gowdy, M. T. Graham, P. Grenier, C. Hast, W. R. Innes, J. Kaminski, M. H. Kelsey, H. Kim, P. Kim, M. L. Kocian, D. W. G. S. Leith, S. Li, B. Lindquist, S. Luitz, V. Luth, H. L. Lynch, D. B. MacFarlane, H. Marsiske, R. Messner, D. R. Muller, H. Neal, S. Nelson, C. P. O'Grady, I. Ofte, A. Perazzo, M. Perl, B. N. Ratcliff, A. Roodman, A. A. Salnikov, R. H. Schindler, J. Schwiening, A. Snyder, D. Su, M. K. Sullivan, K. Suzuki, S. K. Swain, J. M. Thompson, J. Va'vra, A. P. Wagner, M. Weaver, C. A. West, W. J. Wisniewski, M. Wittgen, D. H. Wright, H. W. Wulsin, A. K. Yarritu, K. Yi, C. C. Young, V. Ziegler

Stanford Linear Accelerator Center, Stanford, California 94309, USA

---

[7]Also with Università di Sassari, Sassari, Italy

P. R. Burchat, A. J. Edwards, S. A. Majewski, T. S. Miyashita, B. A. Petersen, L. Wilden

Stanford University, Stanford, California 94305-4060, USA

S. Ahmed, M. S. Alam, J. A. Ernst, B. Pan, M. A. Saeed, S. B. Zain

State University of New York, Albany, New York 12222, USA

S. M. Spanier, B. J. Wogsland

University of Tennessee, Knoxville, Tennessee 37996, USA

R. Eckmann, J. L. Ritchie, A. M. Ruland, C. J. Schilling, R. F. Schwitters

University of Texas at Austin, Austin, Texas 78712, USA

B. W. Drummond, J. M. Izen, X. C. Lou

University of Texas at Dallas, Richardson, Texas 75083, USA

F. Bianchi[ab], D. Gamba[ab], M. Pelliccioni[ab]

INFN Sezione di Torino[a]; Dipartimento di Fisica Sperimentale, Università di Torino[b], I-10125 Torino, Italy

M. Bomben[ab], L. Bosisio[ab], C. Cartaro[ab], G. Della Ricca[ab], L. Lanceri[ab], L. Vitale[ab]

INFN Sezione di Trieste[a]; Dipartimento di Fisica, Università di Trieste[b], I-34127 Trieste, Italy

V. Azzolini, N. Lopez-March, F. Martinez-Vidal, D. A. Milanes, A. Oyanguren

IFIC, Universitat de Valencia-CSIC, E-46071 Valencia, Spain

J. Albert, Sw. Banerjee, B. Bhuyan, H. H. F. Choi, K. Hamano, R. Kowalewski, M. J. Lewczuk, I. M. Nugent, J. M. Roney, R. J. Sobie

University of Victoria, Victoria, British Columbia, Canada V8W 3P6

T. J. Gershon, P. F. Harrison, J. Ilic, T. E. Latham, G. B. Mohanty

Department of Physics, University of Warwick, Coventry CV4 7AL, United Kingdom

H. R. Band, X. Chen, S. Dasu, K. T. Flood, Y. Pan, M. Pierini, R. Prepost, C. O. Vuosalo, S. L. Wu

University of Wisconsin, Madison, Wisconsin 53706, USA

1 INTRODUCTION

The search for the origin of mass is one of the great quests in particle physics. Within the Standard Model [1], fermion and gauge boson masses are generated by the Higgs mechanism through the spontaneous breaking of the electroweak symmetry. A single Standard Model Higgs boson is required to be heavy, with the mass constrained by direct searches to $m_H > 114.4$ GeV [2], and by precision electroweak measurements to $m_H = 129^{+74}_{-49}$ GeV [3].

The Standard Model and the simplest electroweak symmetry breaking scenario suffer from quadratic divergences in the radiative corrections to the mass parameter of the Higgs potential. Several theories beyond the Standard Model that regulate these divergences have been proposed. Supersymmetry [4] is one such model; however, in its simplest form (the Minimal Supersymmetric Standard Model, MSSM) questions of parameter fine-tuning and "naturalness" of the Higgs mass scale remain.

Theoretical efforts to solve unattractive features of MSSM often result in models that introduce additional Higgs fields, with one of them naturally light. For instance, the Next-to-Minimal Supersymmetric Standard Model (NMSSM) [5] introduces a singlet Higgs field. A linear combination of this singlet state with a member of the electroweak doublet produces a CP-odd Higgs state A^0 whose mass is not required to be large. Direct searches typically constrain $m(A^0)$ to be below $2m_b$ [6] making it accessible to decays of Υ resonances. An ideal place to search for such CP-odd Higgs would be $\Upsilon \to \gamma A^0$, as originally proposed by Wilczek [7]. A study of the NMSSM parameter space [8] predicts the branching fraction to this final state to be as high as 10^{-4}.

The decays of the light Higgs boson depend on its mass and couplings, as well as on the low-energy particle spectrum of the underlying theory. In certain NMSSM scenarios, particularly those in which the mass of the lightest supersymmetric particle (LSP) is above m_τ or if $m_{A^0} < 2m_\tau$, the dominant decay mode of A^0 may be invisible: $A^0 \to \chi^0 \bar{\chi}^0$, where the neutralino χ^0 is the LSP. The cleanest experimental signature of such decays is production of monochromatic single photons in decays $\Upsilon \to \gamma A^0$, accompanied by a significant missing energy and momentum. The photon energy in the Υ center-of-mass (CM) [8] is given by

$$E^*_\gamma = \frac{m^2_\Upsilon - m^2_{A^0}}{2m_\Upsilon} \; . \tag{1}$$

The current best limit on the branching fraction $\mathcal{B}(\Upsilon \to \gamma X)$ with $X \to$ invisible comes from a measurement by the CLEO collaboration on $\Upsilon(1S)$ [9]. The quoted limits range from 1.3×10^{-5} for the lightest m_X (highest-energy photons) to $(4\text{–}6) \times 10^{-4}$ for $m_X \approx 8$ GeV (PDG quotes this result as $\mathcal{B}(\Upsilon(1S) \to \gamma X) < 3 \times 10^{-5}$ for $m_X < 7.2$ GeV [10]). There are currently no competitive measurements at the higher-mass Υ resonances.

In the following, we describe a search for a monochromatic peak in the missing mass distribution of events with a single high-energy photon. We assume that the decay width of A^0 is negligibly small compared to experimental resolution, as expected [11] for m_{A^0} sufficiently far from the mass of η_b [12]. Furthermore, we assume that a single A^0 state exists in the range $0 < m_{A^0} \leq 7.8$ GeV; or if two or more states are present, they do not interfere.

---

[8]Hereafter $*$ denotes a CM quantity

2 THE *BABAR* DETECTOR AND DATASET

We search for two-body transitions $\Upsilon(3S) \to \gamma A^0$, followed by invisible decays of A^0 in a sample of $(121.8 \pm 1.2) \times 10^6$ $\Upsilon(3S)$ decays collected with the *BABAR* detector at the PEP-II asymmetric-energy e^+e^- collider at the Stanford Linear Accelerator Center. The data were collected at the nominal CM energy $E_{cm} = 10.355$ GeV. The CM frame was boosted relative to the detector approximately along the detector's magnetic field axis by $\beta_z = 0.469$.

For characterization of the background events we also use a sample of 0.97 fb^{-1} collected 30 MeV below the $\Upsilon(2S)$ resonance, a sample of 2.6 fb^{-1} collected 30 MeV below the $\Upsilon(3S)$ resonance, $\Upsilon(4S)$ decays corresponding to the integrated luminosity of 4.7 fb^{-1}, and 4.5 fb^{-1} integrated above the $\Upsilon(4S)$ resonance. We henceforth refer to these datasets as the *off-resonance* sample.

Since the *BABAR* detector is described in detail elsewhere [13], only the components of the detector crucial to this analysis are summarized below. Charged particle tracking is provided by a five-layer double-sided silicon vertex tracker (SVT) and a 40-layer drift chamber (DCH). Photons and neutral pions are identified and measured using the electromagnetic calorimeter (EMC), which comprises 6580 thallium-doped CsI crystals. These systems are mounted inside a 1.5-T solenoidal superconducting magnet. The Instrumented Flux Return (IFR) forms the return yoke of the superconducting coil, instrumented in the central barrel region with limited streamer tubes for the identification of muons and the detection of clusters produced by neutral hadrons. We use the GEANT [14] software to simulate interactions of particles traversing the *BABAR* detector, taking into account the varying detector conditions and beam backgrounds.

3 SINGLE PHOTON TRIGGER

Detection of the low-multiplicity single photon events requires dedicated trigger and filter lines. Event processing and selection proceeds in three steps. First, the hardware-based Level-1 (L1) trigger accepts single-photon events if they contain at least one EMC cluster with energy above 800 MeV (in the laboratory frame). The total L1 trigger rate was typically 4–5 kHz for a combination of 24 trigger topologies, including the single-photon line which contributed the rate of 300–400 Hz. Second, L1-accepted events are forwarded to a software-based Level-3 (L3) trigger, which forms DCH tracks and EMC clusters and makes decisions for a variety of physics signatures. Two single-photon L3 trigger lines were active during the data taking period. The high-energy ("HighE") line requires an isolated EMC cluster with CM energy $E_\gamma^* > 2$ GeV, and no tracks originating from the e^+e^- interaction region. A subset of the data, amounting to $(82.8 \pm 0.8) \times 10^6$ $\Upsilon(3S)$ decays and 2.6 fb^{-1} collected 30 MeV below the $\Upsilon(3S)$, were also processed with a low-energy ("LowE") single-photon trigger, which requires an EMC cluster with CM energy $E_\gamma^* > 1$ GeV, and no tracks originating from the e^+e^- interaction region. The acceptance rate of the two single-photon L3 lines was up to 100 Hz. Events accepted by L3 are written to mass storage, at the rate of up to 900 Hz.

Additional requirements are applied to the events at the reconstruction stage. We process single-photon events if they satisfy one of the two criteria. The "HighE" selection requires one EMC cluster in the event with a CM energy $E_\gamma^* > 3$ GeV and no DCH tracks with momentum $p^* > 1$ GeV. The "LowE" selection requires one EMC cluster with the transverse profile consistent with an electromagnetic shower and a CM energy $E_\gamma^* > 1.5$ GeV, and no DCH tracks with momentum $p^* > 0.1$ GeV. The two selection criteria are not mutually exclusive.

4 EVENT SELECTION AND YIELDS

Due to the specifics of the online and reconstruction selections, we split the dataset into two broad energy ranges based on the energy of the highest-energy (in the CM frame) EMC cluster. The high-energy region, accepted by "HighE" L3 and reconstruction selections, corresponds to $3.2 < E_\gamma^* < 5.5$ GeV. The backgrounds in this region are dominated by the QED process $e^+e^- \to \gamma\gamma$, especially near $E_\gamma^* = E_{cm}/2$, where the photon energy distribution for $e^+e^- \to \gamma\gamma$ events peaks. The offline event selection is optimized to reduce this peaking background as much as possible.

The second energy range is $2.2 < E_\gamma^* < 3.7$ GeV, which corresponds to the "LowE" online selection. This region is dominated by the low-angle radiative Bhabha events $e^+e^- \to e^+e^-\gamma$, in which both electron and positron miss the sensitive detector volumes. In the region $3.0 < E_\gamma^* < 3.7$ GeV, the tail from the $e^+e^- \to \gamma\gamma$ background is significant.

A limited number of variables are available for these very low-multiplicity event samples. We use the following variables to select the events of interest:

- Photon quality: number of crystals in the EMC cluster N_{crys}, and transverse shower moments LAT and a_{42} [15].

- Fiducial selection of the primary photons: cosine of the CM polar angle $\cos\theta_\gamma^*$ and the azimuthal angle ϕ_γ^*. The signal photons are expected to be distributed as $1 + \cos^2\theta^*$, while the backgrounds are more strongly peaked in the forward and backward directions.

- Extra particles in the event: we require that no charged-particle tracks are found in the SVT and the DCH. We also apply cuts on the energy of the second-highest photon in the event E_2^* (computed in CM frame), extra energy in the calorimeter $E_{\mathrm{extra}} = E_{\mathrm{total}} - E_\gamma$, computed in the lab frame, and the azimuthal angle difference between the primary and the second photon in the event $\phi_2^* - \phi_1^*$. Non-zero E_{extra} may be present in the signal events due to machine backgrounds. The cut on $\phi_2^* - \phi_1^*$ suppresses $e^+e^- \to \gamma\gamma$ and other QED backgrounds.

- IFR veto: we cut on the azimuthal angle difference between the primary photon and any IFR cluster. This variable, $\Delta\phi_{\mathrm{NH}}^*$, rejects the $e^+e^- \to \gamma\gamma$ events in which one of the photons is lost in the dead regions between the EMC crystals, but is reconstructed as an IFR cluster.

We optimize the event selection to maximize $\varepsilon_S/\sqrt{\varepsilon_B}$, where ε_S is the selection efficiency for the signal, and ε_B is the background efficiency. We use Monte Carlo samples generated over a broad range $0 < m_{A^0} \leq 8$ GeV of possible A^0 masses for the signal events. We also use approximately 10% of the available dataset as a background sample for the selection optimization. This sample is included in the final fit.

In the following, we present the analysis of the data in each energy range separately. We use the high-energy region to measure the signal yields in the mass range $0 < m_{A^0} \leq 6$ GeV. We measure the yields in the region $6 < m_{A^0} \leq 7.8$ GeV using the low-energy region. The overlap between the two regions is minimal, and the events yields are consistent in the range of m_{A^0} where the regions overlap.

4.1 HIGH-ENERGY REGION

The final selection for the energy range $3.2 < E_\gamma^* < 5.5$ GeV is summarized in Table 1. The selection efficiency for signal is 10-11%, depending on m_{A^0}, and is below 10^{-5} for $e^+e^- \to \gamma\gamma$ events. Most of the signal efficiency loss occurs due to the fiducial requirements: the CM polar angle selection

Table 1: Selection criteria for the two regions, low and high energies.

Variable	$3.2 < E_\gamma^* < 5.5$ GeV	$2.2 < E_\gamma^* < 3.7$ GeV
Number of crystals in EMC cluster	$20 < N_{\text{crys}} < 48$	$12 < N_{\text{crys}} < 36$
LAT shower shape	$0.24 < LAT < 0.51$	$0.15 < LAT < 0.49$
a_{42} shower shape	$a_{42} < 0.07$	$a_{42} < 0.07$
Polar angle acceptance	$-0.31 < \cos\theta_\gamma^* < 0.6$	$-0.46 < \cos\theta_\gamma^* < 0.46$
2nd highest cluster energy (CMS)	$E_2^* < 0.2$ GeV	$E_2^* < 0.14$ GeV
Extra photon correlation	$\cos(\phi_2^* - \phi_1^*) > -0.95$	$\cos(\phi_2^* - \phi_1^*) > -0.95$
Extra EMC energy (Lab)	$E_{\text{extra}} < 0.1$ GeV	$E_{\text{extra}} < 0.22$ GeV
IFR veto	$\cos(\Delta\phi_{\text{NH}}^*) > -0.9$	$\cos(\Delta\phi_{\text{NH}}^*) > -0.95$
IFR fiducial	$\cos(6\phi_\gamma^*) < 0.96$	...

$-0.31 < \cos\theta_\gamma^* < 0.6$ ensures that the second photon from $e^+e^- \to \gamma\gamma$ background would hit the barrel regions of the EMC and the IFR, and the azimuthal requirement $\cos(6\phi_\gamma^*) < 0.96$ vetoes the dead regions between the six equal-size IFR sectors.

We extract the yield of signal events as a function of the assumed mass m_{A^0} in the interval $0 < m_{A^0} \leq 6$ GeV by performing a series of unbinned extended maximum likelihood fits to the distribution of the missing mass squared

$$m_X^2 \equiv m_{\Upsilon(3S)}^2 - 2E_\gamma^* m_{\Upsilon(3S)} \tag{2}$$

in fine steps of $\Delta m_{A^0} = 0.1$ GeV. After the final selection, 955 events remain in the data sample in the interval $-5 \leq m_X^2 \leq 40$ GeV^2. The dominant background in this region is from $e^+e^- \to \gamma\gamma$, radiative Bhabha, and two-photon fusion events. The background from $e^+e^- \to \gamma\gamma$ is particularly problematic, since its distribution peaks near $m_X^2 = 0$. We determine the probability density function (PDF) of this background by selecting a high-statistics sample of on-resonance $e^+e^- \to \gamma\gamma$ events with the IFR veto removed (a total of 244,462 events). We determine the efficiency of the IFR veto by selecting $e^+e^- \to \gamma\gamma$ events with one photon in the off-resonance sample. We find $\varepsilon_{\text{IFR veto}} = N_{\gamma\gamma\,\text{veto}}/N_{\gamma\gamma\,\text{no veto}} = (4.5 \pm 1.9) \times 10^{-4}$, where $N_{\gamma\gamma\,\text{veto}}$ is the number of events accepted with the full selection (Table 1), and $N_{\gamma\gamma\,\text{no veto}}$ is the number of events accepted with the same selection but IFR veto removed. The uncertainty accounts for the time-dependent variation in $\varepsilon_{\text{IFR veto}}$ between the different off-resonance samples. We then fix the number of expected $e^+e^- \to \gamma\gamma$ events to $N_{\gamma\gamma} = 110 \pm 46$.

The background from the radiative Bhabha and two-photon fusion events is described by a smooth exponential function $f_{\text{bkg}}(m_X^2) \propto \exp(cm_X^2)$. The parameter c and the yield of this continuum background are left free in the fit.

Our Monte Carlo simulations estimate that the backgrounds from the generic $\Upsilon(3S)$ decays or misreconstructed vector mesons produced through initial-state radiation (ISR) processes are negligible. The ISR processes can potentially contribute peaking backgrounds at low m_X^2. We see no evidence for these extra contributions in the off-resonance sample, but also vary the peaking $e^+e^- \to \gamma\gamma$ PDF to estimate potential systematic effects.

The signal PDF is described by a Crystal Ball [16] function centered around the expected value of $m_X^2 = m_{A^0}^2$. We determine the PDF as a function of m_{A^0} using high-statistics simulated samples of signal events, and we determine the uncertainty in the PDF parameters by comparing
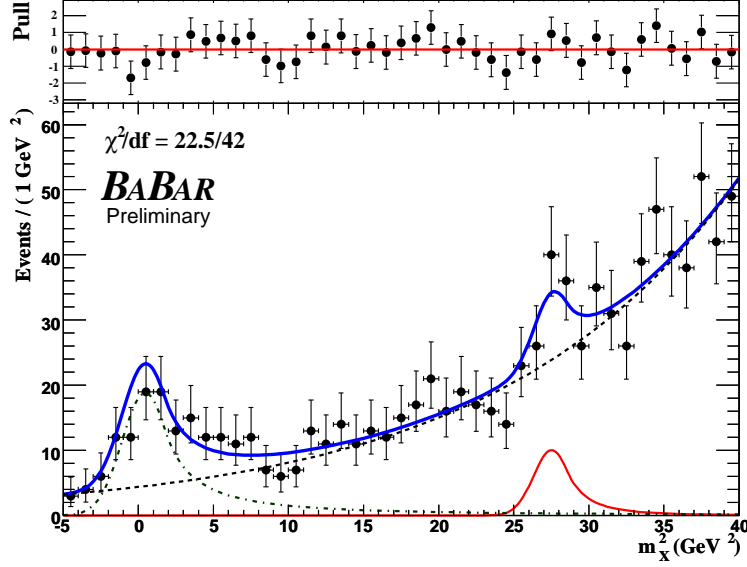
11

Figure 1: Sample fit to the high-energy dataset ($122 \times 10^6 \; \Upsilon(3S)$ decays). The bottom plot shows the data (solid points) overlaid by the full PDF curve (solid blue line), signal contribution with $m_{A^0} = 5.2$ GeV (solid red line), $e^+e^- \to \gamma\gamma$ contribution (dot-dashed green line), and continuum background PDF (black dashed line). The top plot shows the pulls $p = (\text{data} - \text{fit})/\sigma(\text{data})$ with unit error bars.
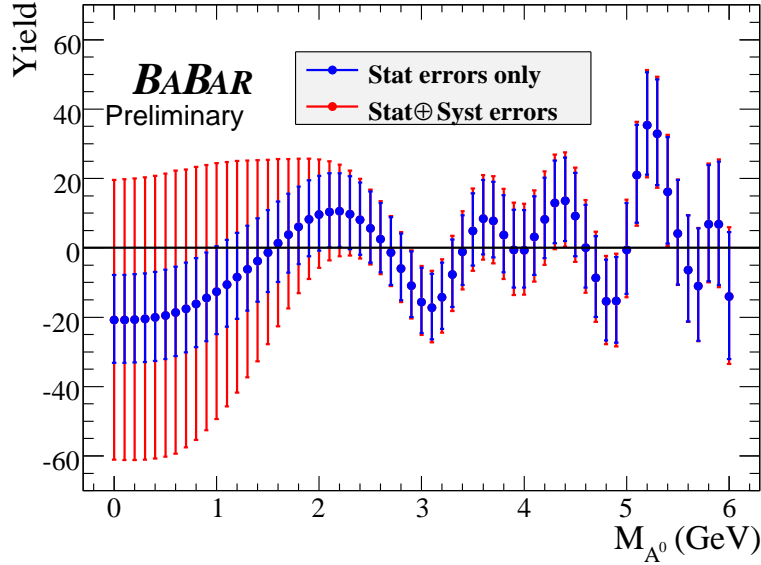

Figure 2: Signal yields N_{sig} as a function of assumed mass m_{A^0} in the high-energy dataset. Blue error bars are statistical only, and the red error bars include the systematic contributions. Since the spacing between the points is smaller than the experimental resolution, the neighboring points are highly correlated.

the distributions of the simulated and reconstructed $e^+e^- \rightarrow \gamma\gamma$ events. The resolution for signal events varies between $\sigma(m_X^2) = 1.5$ GeV^2 for $m_{A^0} \approx 0$ to $\sigma(m_X^2) = 0.7$ GeV^2 for $m_{A^0} = 8$ GeV.

A sample fit, for $m_{A^0} = 5.2$ GeV, is shown in Fig. 1. This fit corresponds to the signal yield of $N_{sig} = 37 \pm 15$, with the statistical significance of $\mathcal{S} \equiv \sqrt{2 \ln(L_{max}/L_0)} = 2.6\sigma$, where L_{max} is the maximum value of the likelihood, and L_0 is the value of the likelihood with the signal yield fixed to zero. No other values of $m_{A^0} < 6$ GeV return higher significance or likelihood. The results of the fits in fine steps of m_{A^0} are shown in Fig. 2.

4.2   LOW-ENERGY REGION

The final selection for the energy range $2.2 < E_\gamma^* < 3.7$ GeV is summarized in Table 1. The selection efficiency for signal is 20%. Most of the signal efficiency loss occurs due to the fiducial requirement on the CM polar angle $|\cos\theta_\gamma^*| < 0.46$, applied to suppress the background from $e^+e^- \rightarrow e^+e^-\gamma$, which rises steeply in the forward and backward directions. We restrict the photon energy range to avoid the region $E_\gamma^* < 2.2$ GeV where the backgrounds are excessively high and the single-photon trigger selection requires further investigation.

We extract the yield of the signal events as a function of the assumed mass m_{A^0} in the range $6 < m_{A^0} \leq 7.8$ GeV by performing a set of unbinned extended maximum likelihood fits to the distribution of the missing mass squared m_X^2 in steps of $\Delta m_{A^0} = 0.025$ GeV. After the final selection, 14,947 events remain in the data sample in the interval $30 \leq m_X^2 \leq 62$ GeV^2. The dominant background in this region is from the radiative Bhabha $e^+e^- \rightarrow e^+e^-\gamma$ events, with contributions from $e^+e^- \rightarrow \gamma\gamma$ becoming relevant at low values of m_X^2 (high photon energy).

We parameterize the background from the radiative Bhabha events by a smooth exponential function $f_{Bhabha}(m_X^2) \propto \exp(c_1 m_X^2 + c_2 m_X^4)$. The parameters c_1 and c_2, as well as the yield of $e^+e^- \rightarrow e^+e^-\gamma$ events are left free in the fit. This PDF also accounts for other radiative processes, such as $e^+e^- \rightarrow \tau^+\tau^-\gamma$ and $e^+e^- \rightarrow \mu^+\mu^-\gamma$.

The $e^+e^- \rightarrow \gamma\gamma$ distribution is modeled by a sample of simulated events with an equivalent integrated luminosity of 22 fb^{-1}. The PDF has two components: a smooth continuum with a turn-on of $e^+e^- \rightarrow 3\gamma$ events starting around $m_X^2 = 53$ GeV^2, and a broad peak with the width of about 2.5 GeV^2 which accounts for a forward and backward corner of 3γ phase space. The fraction of this peak, the fraction of the continuum $e^+e^- \rightarrow 3\gamma$ events, and the normalization of the $e^+e^- \rightarrow \gamma\gamma(\gamma)$ events are left free in the fit. The signal PDF is described by the same Crystal Ball [16] function as in the high-energy region.

A fit for $m_{A^0} = 7.275$ GeV, is shown in Fig. 3. This fit corresponds to the signal yield of $N_{sig} = 119 \pm 71$, with statistical significance of $\mathcal{S} \equiv \sqrt{2 \ln(L_{max}/L_0)} = 1.7\sigma$. No other values in the range $6 < m_{A^0} \leq 7.8$ GeV return higher significance. This fit also returns $N_{Bhabha} = 11419 \pm 441$ and $N_{\gamma\gamma} = 3410 \pm 451$. The results of the fits in fine steps of m_{A^0} are shown in Fig. 4. For each fit where the signal yield is allowed to vary, we also allow for the variation of the background shape parameters. We find that the shapes of the background PDFs are independent of the assumed m_{A^0}, and is also consistent with the distribution in the off-resonance sample. We observe no significant excess of events over the range $6 < m_{A^0} \leq 7.8$ GeV.

5   SYSTEMATIC UNCERTAINTIES

The largest systematic uncertainties in the signal yield come from the estimate of the $e^+e^- \rightarrow \gamma\gamma$ peaking background yield in the high-energy region and its shape (in both energy regions). Varying
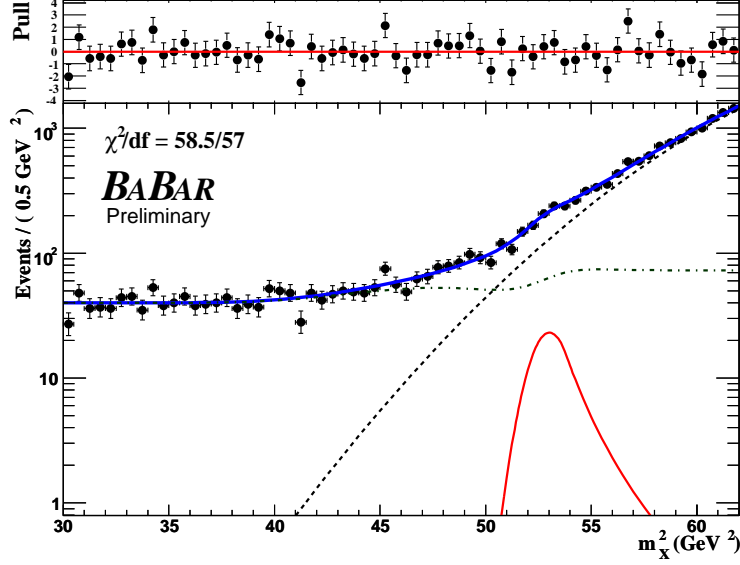
Figure 3: Sample fit to the low-energy dataset (83×10^6 $\Upsilon(3S)$ decays). The bottom plot shows the data (solid points) overlaid by the full PDF curve (solid blue line), signal contribution with $m_{A^0} = 7.275$ GeV (solid red line), $e^+e^- \to \gamma\gamma$ contribution (dot-dashed green line), and continuum background PDF (black dashed line). The top plot shows the pulls $p = (\text{data} - \text{fit})/\sigma(\text{data})$ with unit error bars.
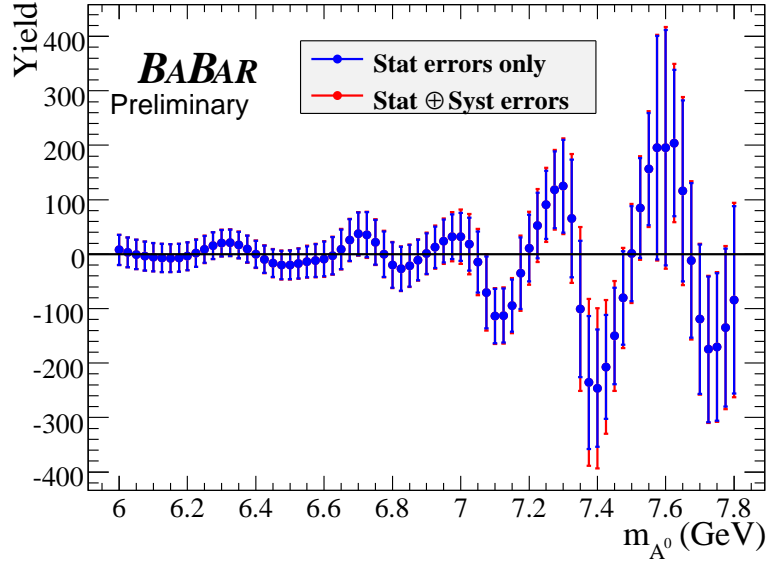

Figure 4: Signal yields N_{sig} as a function of assumed mass m_{A^0} in the "LowE" region. Blue error bars are statistical only, and the red error bars include the systematic contributions. Since the spacing between the points is smaller than the experimental resolution, the neighboring points are highly correlated.

the peaking $e^+e^- \to \gamma\gamma$ background contribution by its uncertainty changes the signal yield by ± 38 events for $m_{A^0} = 0$, with the effect decreasing with increased m_{A^0}. The uncertainty due to the $e^+e^- \to \gamma\gamma$ PDF is largest in the low-energy region, where it contributes up to ± 70 events (for $m_{A^0} = 7.4$ GeV) to the uncertainty in the signal yield.

We determine the uncertainty in the signal PDF by comparing the data and simulated distributions of $e^+e^- \to \gamma\gamma$ events. We correct for the differences observed, and use half of the correction as an estimate of the systematic uncertainty. The effect on the signal yield is generally small, except for the region near $m_{A^0} = 7.4$ GeV, where the systematic variation of the signal PDF changes the yield by ± 64 events. Such large variation is caused by high correlation with the $e^+e^- \to \gamma\gamma$ yield in this region. The total additive systematic uncertainty on the yield is ranges between 1 and 100 events, depending on m_{A^0}.

We measure the trigger and filter selection efficiency using single-photon $e^+e^- \to \gamma\gamma$ and $e^+e^- \to e^+e^-\gamma$ events selected from a sample of unbiased randomly accepted triggers. We find excellent agreement with the Monte Carlo estimates of the trigger efficiency, within the systematic uncertainty of 0.4%. We measure the efficiency of single photon reconstruction in a large sample of $e^+e^- \to \mu^+\mu^-\gamma$, $e^+e^- \to \tau^+\tau^-\gamma$, and $e^+e^- \to \gamma\omega$ events, and assign a systematic uncertainty on the reconstruction efficiency of 2%. We assign an additional 2% systematic uncertainty on the single photon selection. The uncertainty on the total number of recorded $\Upsilon(3S)$ decays is estimated to be 1.1%. The total multiplicative error on the branching fraction is 3.1%.

6   RESULTS AND CONCLUSIONS

We do not observe a significant excess of events above the background in the range $0 < m_{A^0} \leq 7.8$ GeV, and set upper limits on the branching fraction $\mathcal{B}(\Upsilon(3S) \to \gamma A^0) \times \mathcal{B}(A^0 \to \text{invisible})$. We add statistical and systematic uncertainties (which include the additive errors on the signal yield and multiplicative uncertainties on the signal efficiency and the number of recorded $\Upsilon(3S)$ decays) in quadrature. The 90% C.L. Bayesian upper limits, computed with a uniform prior and assuming a Gaussian likelihood function, are shown in Fig. 5 as a function of mass m_{A^0}. The limits range from 0.7×10^{-6} (at $m_{A^0} = 3.0$ GeV) to 31×10^{-6} (at $m_{A^0} = 7.6$ GeV). These results are preliminary.
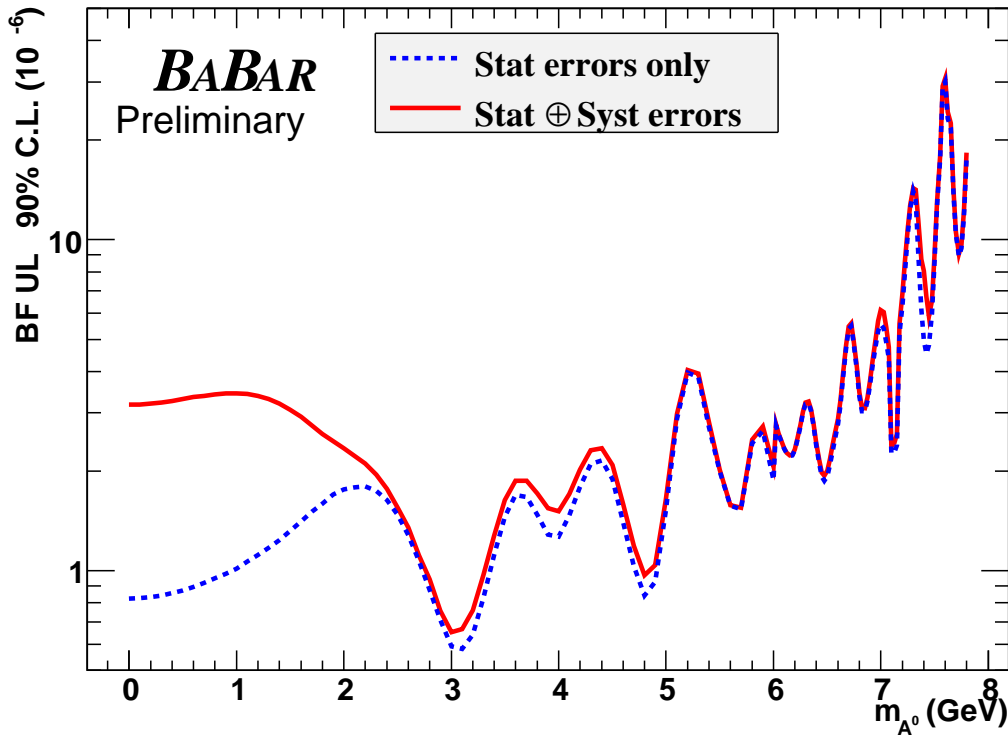
7   ACKNOWLEDGMENTS

Figure 5: 90% C.L. upper limits on the branching fraction $\mathcal{B}(\Upsilon(3S) \to \gamma A^0) \times \mathcal{B}(A^0 \to \text{invisible})$. The dashed blue line shows the statistical uncertainties only, the solid red line includes the systematic uncertainties.

References

[1] S. Weinberg, Phys. Rev. Lett. **19**, 1264 (1967); A. Salam, p. 367 of *Elementary Particle Theory*, ed. N. Svartholm (Almquist and Wiksells, Stockholm, 1969); S.L. Glashow, J. Iliopoulos, and L. Maiani, Phys. Rev. D **2**, 1285 (1970).

[2] LEP Working Group for Higgs boson searches, R. Barate *et al.*, Phys. Lett. **B565**, 61 (2003).

[3] LEP-SLC Electroweak Working Group, Phys. Rept. **427**, 257 (2006).

[4] J. Wess and B. Zumino, Nucl. Phys. **B70**, 39 (1974).

[5] R. Dermisek and J.F. Gunion, Phys. Rev. Lett. **95**, 041801 (2005).

[6] R. Dermisek and J.F. Gunion, Phys. Rev. D **73**, 111701 (2006).

[7] F. Wilczek, Phys. Rev. Lett. **39**, 1304 (1977).

[8] R. Dermisek, J.F. Gunion, and B. McElrath, Phys. Rev. D **76**, 051105 (2007).

[9] CLEO Collaboration, R. Balest *et al.*, Phys. Rev. D **51**, 2053 (1995).

[10] Particle Data Group, W.-M. Yao *et al.*, J. Phys. G **33**, 1 (2006).

[11] E. Fullana and M.A. Sanchis-Lozano, Phys. Lett. B **653**, 67 (2007).

[12] *BABAR* Collaboration, B. Aubert *et al.*, preprint arXiv:0807.1086 [hep-ex], accepted to Phys. Rev. Lett.

[13] *BABAR* Collaboration, B. Aubert *et al.*, Nucl. Instrum. Methods Phys. Res., Sect. A **479**, 1 (2002).

[14] GEANT4 Collaboration, S. Agostinelli *et al.*, Nucl. Instrum. Methods Phys. Res., Sect. A **506**, 250 (2003).

[15] ARGUS Collaboration, A. Drescher *et al.*, Nucl. Instrum. Methods Phys. Res., Sect. A **237**, 464 (1985).

[16] M. J. Oreglia, Ph.D Thesis, report SLAC-236 (1980), Appendix D; J. E. Gaiser, Ph.D Thesis, report SLAC-255 (1982), Appendix F; T. Skwarnicki, Ph.D Thesis, report DESY F31-86-02(1986), Appendix E.